

Polarized Raman Spectroscopy of Bone Tissue: Watch the Scattering

Mekhala Raghavan^a, Nadder D. Sahar^a, Robert H. Wilson^b, Mary-Ann Mycek^{a,b,c}, Nancy Pleshko^d,
David H. Kohn^{a,e,f}, Michael D. Morris^g

^aDepartment of Biomedical Engineering, University of Michigan, Ann Arbor, MI USA 48109-2099

^bApplied Physics Program, University of Michigan, Ann Arbor, MI, USA

^cComprehensive Cancer Center, University of Michigan, Ann Arbor, MI, USA

^dDepartment of Mechanical Engineering, Temple University, Philadelphia, PA, USA

^eDepartment of Biologic and Materials Sciences, University of Michigan, Ann Arbor, MI USA

^fSchool of Dentistry, University of Michigan, Ann Arbor, MI, USA

^gDepartment of Chemistry, University of Michigan, Ann Arbor, MI USA 48109-1055

ABSTRACT

Polarized Raman spectroscopy is widely used in the study of molecular composition and orientation in synthetic and natural polymer systems. Here, we describe the use of Raman spectroscopy to extract quantitative orientation information from bone tissue. Bone tissue poses special challenges to the use of polarized Raman spectroscopy for measurement of orientation distribution functions because the tissue is turbid and birefringent. Multiple scattering in turbid media depolarizes light and is potentially a source of error.

Using a Raman microprobe, we show that repeating the measurements with a series of objectives of differing numerical apertures can be used to assess the contributions of sample turbidity and depth of field to the calculated orientation distribution functions. With this test, an optic can be chosen to minimize the systematic errors introduced by multiple scattering events. With adequate knowledge of the optical properties of these bone tissues, we can determine if elastic light scattering affects the polarized Raman measurements.

Keywords: Raman spectroscopy, bone, polarization, light scattering

1. INTRODUCTION

Raman microspectroscopy has been established as a powerful tool for monitoring molecular deformation in a range of natural and synthetic crystalline materials and polymers.⁽¹⁾ Polarized Raman spectroscopy has been an often used tool to study orientation in crystalline solids⁽²⁾ and in both natural and synthetic fibers at the ultrastructural level.⁽³⁾ In crystals, when molecular orientation is known relative to the polarization of the laser beam, the depolarization ratio is strongly influenced by molecular alignment; therefore, it can provide additional structural information. In the mineralized tissue literature, the first use of polarized Raman spectroscopy was to study dental enamel crystallite orientation.⁽⁴⁾ It has also been employed to examine healthy⁽⁵⁾ and carious⁽⁶⁾ enamel.

It is well-known that the organization of the bone ultrastructure i.e., the collagen orientation and mineral crystal alignment influence the mechanical behavior of bone.⁽⁷⁾ Recently, qualitative polarized Raman spectroscopic imaging has been used by Kazanci et al. to study the orientation and composition of cortical bone tissue.^(8, 9) The study demonstrated that the orientation of both mineral and collagen can be elucidated by examining the polarization components of phosphate ν_1 (P-O symmetric stretch) and amide I (carbonyl stretch). These workers pointed out that because the crystallites are oriented with their c-axes along the length of collagen fibrils phosphate ν_1 should be strongly polarized along this axis. Similarly, because the carbonyl groups are oriented perpendicular to the collagen chain, amide I is strongly polarized in the direction perpendicular to the collagen fibril orientation.

In the present study, we extend the polarized Raman microspectroscopy technique to extract quantitative orientation information from bone tissue. Because bone tissue is optically thick, birefringent and highly turbid, light will be scattered as it travels through bone. Hence, polarized light will be partially or completely depolarized by multiple elastic scattering as it travels deeper in the tissue. We show that repeating the polarized Raman measurements with a series of objectives of differing numerical apertures can be used to assess the contributions of sample turbidity and depth of field on the depolarization ratios. Because the measured depolarization ratios are used to calculate the orientation order parameters which define the molecular orientation function, it is important to minimize the effects of multiple elastic scattering on the polarized Raman measurements.

2. METHODOLOGY

2.1 Materials

Murine femora from 5-week old female wild type mice and 5-week old female *oim/oim* mice were used. The mice were part of a larger IACUC-approved study at the Hospital for Special Surgery. The wild type femora were significantly heavier (42.7 ± 2.14 mg) and had larger cross-sections (1.37 ± 0.06 mm) than that of the *oim/oim* mice femora (34.1 ± 2.7 mg and 1.25 ± 0.08 mm). The *oim/oim* bones are deficient in $\text{pro}\alpha 2(\text{I})$ collagen which leads to an increased susceptibility to fracture.⁽¹⁰⁾ Small angle X-ray scattering studies have shown that mineral crystals are less well aligned in the *oim/oim* mice relative to the heterozygotes.⁽¹¹⁾ The femora were immersed in phosphate buffered saline (PBS) and frozen until use. The specimens were thawed to room temperature before collection of spectra and kept moist throughout an experiment.

2.2 Elastic Light Scattering & Polarized Raman Spectroscopy

To quantify elastic scattering in the wild type and *oim/oim* bone specimens, the reduced scattering coefficient of each specimen ($\mu_s' = \mu_s(1-g)$, where μ_s is the scattering coefficient and g is the anisotropy) was measured. For this purpose, an integrating sphere (RT-060-SF, Labsphere) connected to a spectrograph (HR2000+, Ocean Optics) was employed. A lamp attached to a Kohler Illuminator (KI-120, Labsphere) and powered by an LPS preset power supply (LPS-150-0660, Labsphere) was used to deliver a uniform beam of light to the bone specimens. The beam diameter ($1 \mu\text{m}$) was controlled by a 1:2 telescope and an adjustable iris. Two-tailed unpaired t-tests were performed to determine if there was a statistically significant difference between the measured reduced scattering coefficients of the wild type and *oim/oim* femora.

Orientation-sensitive polarized Raman spectra of bone were collected from the mid-diaphysis region of wild type ($n=8$) and *oim/oim* ($n=8$) murine femora using a locally-constructed Raman microprobe. The polarization axis of the laser beam and collected Raman scatter were controlled with standard polarization optics. A wedge depolarizer in front of the spectrometer eliminated intensity artifacts caused by the polarization dependence of the grating transmission efficiency. Raman spectra were acquired along both the proximal-distal (x) and medial-lateral (y) directions of the specimens (Figure 1). Depolarization ratios ($R_x = I_{xy}/I_{xx}$ and $R_y = I_{yx}/I_{yy}$) were calculated from the Raman measurements.

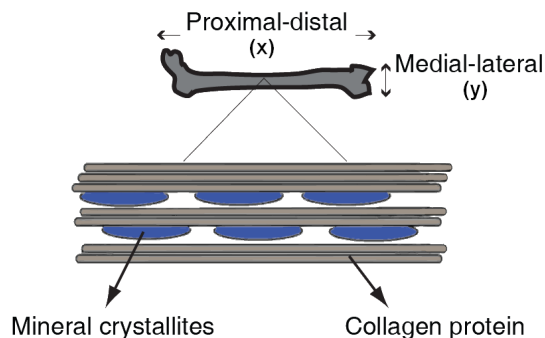


Fig 1. Polarization directions with respect to the long axis of the diaphysis of the bone

To help define the NA needed for artifact-free polarization measurements, the apparent depolarization ratio for phosphate (959 cm^{-1}) was measured on a representative wild type specimen using objectives of increasingly higher NA [4X (0.20 NA), 20X (0.50 NA), 20X (0.75 NA) and 40X (0.90 NA)] to find the values at which the depolarization ratio was independent of NA. Orientational order parameters, P2 and P4, for the phosphate mineral were calculated from the spectra using published mathematical procedures.⁽¹²⁾ With only these order parameters, the orientation distribution function $N(\theta)$ can be predicted as the most probable orientation distribution function using information theory. The limiting values for P₂ are 1 and -0.5 for perfect orientation at 0° and 90° from the axis of reference.

2.3 Data Analysis

The wavenumber scale of the spectrograph was calibrated against the emission lines of a neon lamp discharge. Intensities were corrected for polarization dependence of the optics by calibration against cyclohexane.⁽¹³⁾ The spectra were corrected for spectrograph image curvature and dark current subtraction and white light correction were performed.

For the wild type and *oim/oim* specimens, peak fitting was performed using GRAMS/AI 7.01 (ThermoGalactic) and the intensities of the characteristic mineral band (phosphate ν_1 at 959 cm^{-1}) were measured. The Raman depolarization ratios ($R_x = I_{xy} / I_{xx}$ and $R_y = I_{yx} / I_{yy}$) for the mineral bands were corrected for the influence of sample birefringence (reflectivity, internal field, divergence) by assuming the typical collagen and mineral birefringence values of 3×10^{-3} and 7×10^{-3} respectively.⁽¹⁴⁾ Statistical tests were performed on band intensities and depolarization ratios using two-tailed unpaired t-tests to compare effect of different NA and to compare wild type with *oim/oim* specimens. A value of $p < 0.05$ was considered significant.

3. RESULTS

The mean reduced scattering coefficient, μ_s , was calculated to be $14.7 \pm 1.3\text{ cm}^{-1}$ for wild type specimens and $12.3 \pm 2.0\text{ cm}^{-1}$ for *oim/oim* specimens ($p < 0.05$). Estimating the tissue anisotropy to be 0.9 resulted in scattering coefficients of $\mu_s = 147 \pm 13\text{ cm}^{-1}$ for wild type and $\mu_s = 123 \pm 20\text{ cm}^{-1}$ for *oim/oim* specimens. From these values, we estimate that scattering causes about 10% attenuation at a 4 μm depth of penetration for the *oim/oim* and at 3 μm for the wild type.

We measured depolarization ratios for the phosphate Raman band at 959 cm^{-1} in wild type specimens with objectives of different NA. Because of elastic scattering, extensive depolarization was observed at NA 0.75 or lower and further measurements were made only on objectives with NA 0.8 or above (Table 1).

Table 2 compares the order parameters calculated from the polarized Raman measurements on phosphate band of the wild type and *oim/oim* using a 40X, 0.90 NA objective. The phosphate P₂ value for the wild type group is significantly greater than that of the *oim/oim* group ($p < 0.05$). The order parameter P₂, calculated from the depolarization ratios, can vary between -0.5 (perpendicular orientation) to +1 (parallel orientation), with 0 corresponding to random orientation. Normally, the phosphate group is oriented along the x direction of the bone.

Table 1. Depolarization ratios and order parameter, P₂, of phosphate mineral band as a function of microscope objective NA.

Objective	Depolarization Ratios		Order Parameter P ₂
	R _x	R _y	
4X, 0.20 NA (z _{min} = 60.8 μm)	0.60 \pm 0.2	0.78 \pm 0.1	0.03 \pm 0.02
20X, 0.50 NA (z _{min} = 9.7 μm)	0.26 \pm 0.1	0.36 \pm 0.11	0.06 \pm 0.01
20X, 0.75 NA (z _{min} = 4.3 μm)	0.29 \pm 0.05	0.59 \pm 0.09	0.20 \pm 0.02
40X, 0.90 NA (z _{min} = 3.0 μm)	0.06 \pm 0.03	0.74 \pm 0.1	0.72 \pm 0.06

Table 2. Orientational order parameter, P_2 , of phosphate mineral band for wild type and *oim/oim* bones; 0.90 NA objective (* $p < 0.05$)

Raman bands	Order Parameters	Wild Type Group (Mean + SD)	<i>oim/oim</i> Group (Mean + SD)
Phosphate ν_1	P_2	0.72 ± 0.06	$0.60 \pm 0.06^*$
	P_4	0.58 ± 0.08	0.48 ± 0.06

4. DISCUSSION

As the NA decreases, depolarization by elastic light scattering (translucence) increases and the measured value of P_2 decreases. From the scattering coefficients, elastic light scattering will be observable from light that penetrates even a few microns, although not all of this light will be collected by the objective. Because depth of field increases with $1/(NA)^2$, scattering will degrade orientation measurements made with low NA objectives. Measurements with a 0.90 NA objective gives P_2 values indicating near parallel orientation of mineral crystallites.

Therefore, a 40X, 0.90 NA objective was used for all further measurements. The Raman depolarization ratios for the phosphate mineral band are significantly higher for the *oim/oim* specimen than for the wild type specimen. This results in significantly greater P_2 values for the wild type specimen than for the *oim/oim* specimen (Table 2), implying that mineral crystallites are more well oriented in wild type bone than in *oim/oim* bone. These results are in agreement with small angle X-ray scattering studies that demonstrated a greater variability in mineral crystal alignment in cortical *oim/oim* bones than in wild type bones.⁽¹¹⁾

Elastic light scattering measurements showed a lower reduced scattering coefficient in *oim/oim* bones than in wild type bones. This result makes sense because molecular spacing in collagen fibrils from *oim/oim* mice is larger than that in wildtype mice.⁽¹⁵⁾ The increased scattering (less transparency) in wild type bones introduces systematic errors in to the polarization measurements which result in smaller order parameters when objectives with numerical aperture 0.80 and lower are used. Using a higher NA objective (0.90 NA or higher) minimizes translucence errors and yields accurate molecular orientation information.

We caution that knowledge of the optical properties of the specimens is needed to properly employ polarized Raman spectroscopy to study of molecular orientations in bone tissue.

5. CONCLUSIONS

We employ polarized Raman spectroscopy to extract quantitative orientation information from highly turbid bone tissue. Simultaneous quantitative measurements of both matrix collagen and mineral orientation in intact and disordered bone specimens are possible, but it is necessary to verify that elastic light scattering does not significantly perturb the polarized Raman measurements. In this work, we propose tests to choose the right optics to minimize systematic errors and we perform measurements to assess the effect of elastic light scattering on the polarized Raman measurements.

6. ACKNOWLEDGEMENT

This work has been supported by NIH grant R01 AR052010 to MDM, R01-AR48337 to NP and R01-CA-114542 to M-AM, DoD/US Army grant DAMD17-03-1-0556 to DHK and a University of Michigan Barbour scholarship to MR.

7. REFERENCES

- [1] L. S. Schadler, C. Galiotis "Fundamentals and applications of micro Raman spectroscopy to strain measurements in fibre reinforced composites," *International Materials Reviews* 40(3), 116 (1995)
- [2] D. C. Smith and C. Carabtos-Nédelec, "Raman spectroscopy applied to Crystals: Phenomena and Principles, Concepts and Conventions," in *Handbook of Raman Spectroscopy* I. R. Lewis and H. G. M. Edwards, Eds., pp. 349-422, Marcel Dekker, Inc., New York (2001).
- [3] S. Michielsen, "Application of Raman Spectroscopy to Organic Fibers and Films," in *Handbook of Raman Spectroscopy* I. R. Lewis and H. G. M. Edwards, Eds., pp. 749-798, Marcel Dekker, New York (2001).
- [4] Tsuda and J. Arends, "Orientational micro-Raman spectroscopy on hydroxyapatite single crystals and human enamel crystallites," *Journal of Dental Research* 73(11), 1703-1710 (1994)
- [5] G. Leroy, G. Penel, N. Leroy and E. Brès, "Human tooth enamel: a Raman polarized approach," *Applied Spectroscopy* 56(8), 1030-1034 (2002)
- [6] A. C. T. Ko, L.-P. Choo-Smith, M. Hewko, M. G. Sowa, "Detection of early dental caries using polarized Raman spectroscopy," *Optics express* 14(1), 203 (2006)
- [7] P. Fratzl, S. Gupta, E. P. Paschalis, P. Roschger, "Structure and mechanical quality of the collagen–mineral nanocomposite in bone," *Journal of materials chemistry* 14(14), 2115 (2004)
- [8] M. Kazanci, P. Roschger, E. P. Paschalis, K. Klaushofer and P. Fratzl, "Bone osteonal tissues by Raman spectral mapping: Orientation-composition," *Journal of Structural Biology* 156(3), 489-496 (2006)
- [9] M. Kazanci, H. D. Wagner, N. I. Manjubala, H. S. Gupta, E. Paschalis, P. Roschger and P. Fratzl, "Raman imaging of two orthogonal planes within cortical bone," *Bone* 41(3), 456-461 (2007)
- [10] O. Ljunggren, A. Kindmark, C. Rubin, K. Lindahl, "Osteogenesis imperfecta, pathogenesis and treatment," *Bone* 44(2), S202 (2009)
- [11] P. Fratzl, O. Paris, K. Klaushofer, W. J. Landis, "Bone mineralization in an osteogenesis imperfecta mouse model studied by small-angle X-ray scattering," *J. Clin. Invest.* 97, 396 (1996)
- [12] M. E. Rousseau, T. Lefèvre, L. Beaulieu, T. Asakura, M. Pézolet, "Study of protein conformation and orientation in silkworm and spider silk fibers using Raman microspectroscopy," *Biomacromolecules* 5, 2247-57 (2004)
- [13] M. J. Pelletier, "Effects of temperature on cyclohexane Raman bands," *Appl. Spectrosc.* 53, 1087-96 (1999)
- [14] N. J. Everall, "Measurement of orientation and crystallinity in uniaxially drawn poly(ethylene terephthalate) using polarized confocal Raman microscopy," *Appl. Spectrosc.* 52(12), 1498-1504 (1998)
- [15] D. J. McBride, V. Choe, J. R. Shapiro, B. Brodsky, "Altered collagen structure in mouse tail tendon lacking the alpha 2(1) chain," *J. Mol. Biol.* 270, 275-84 (1997).